



**HAL**  
open science

# Classification of pig myofibres and assessment of post-mortem glycogen depletion according to fibre type by computerized image analysis

Louis Lefaucheur, P. Buche, Patrick Ecolan, M. Lemoing

► **To cite this version:**

Louis Lefaucheur, P. Buche, Patrick Ecolan, M. Lemoing. Classification of pig myofibres and assessment of post-mortem glycogen depletion according to fibre type by computerized image analysis. *Meat Science*, 1992, 32 (3), pp.267-278. hal-02699594

**HAL Id: hal-02699594**

**<https://hal.inrae.fr/hal-02699594v1>**

Submitted on 15 Nov 2023

**HAL** is a multi-disciplinary open access archive for the deposit and dissemination of scientific research documents, whether they are published or not. The documents may come from teaching and research institutions in France or abroad, or from public or private research centers.

L'archive ouverte pluridisciplinaire **HAL**, est destinée au dépôt et à la diffusion de documents scientifiques de niveau recherche, publiés ou non, émanant des établissements d'enseignement et de recherche français ou étrangers, des laboratoires publics ou privés.



## Classification of Pig Myofibres and Assessment of Post-mortem Glycogen Depletion According to Fibre Type by Computerized Image Analysis

L. Lefaucheur,<sup>a</sup> P. Buche,<sup>b</sup> P. Ecolan<sup>a</sup>  
& M. Lemoing<sup>b</sup>

<sup>a</sup>INRA, Station de Recherches Porcines, 35590 St Gilles, France

<sup>b</sup>INRA-ENSA, Laboratoire de Biométrie, 35042 Rennes, France

(Received 6 March 1991; revised version received 22 August 1991;  
accepted 30 August 1991)

### ABSTRACT

*A computer-aided method for muscle fibre type determination and qualitative analysis of glycogen at a cellular level is described. The operational system consists of a microscope, a CCD videocamera, an image analysis card, a colour monitor and a standard workstation computer (32 Mb central memory, 22 mips) running under the UNIX operating system. The programme was developed with 512 × 512 pixel images. Four main steps can be distinguished: digitization, network extraction, network matching and measurement of staining intensities. The data generated for each analysed fibre included, diameter, cross-sectional area, ATPase staining intensity and type. Ten minutes of batch processing and 36-41 min of interactive work were needed to analyse 200-300 fibres. Results have shown that this image analysis system can distinguish four types of myofibres denoted I, IIA, IIB and IIC, on the basis of myosin ATPase sensitivity at three preincubation pH values (4.10, 4.35 and 10.4). Preliminary results have also shown that the image analysis system can be used to measure post-mortem glycogen depletion according to fibre type.*

### INTRODUCTION

Mammalian skeletal muscles are composed of fibres with different properties and they can be classified into groups according to common

biochemical, physiological or functional parameters. Muscle fibre composition is of great importance for meat quality and growth (Lefaucheur, 1990). Numerous classifications are used for the histochemical classification of skeletal muscle fibres (Brooke & Kaiser, 1970; Ashmore & Doerr, 1971; Peter *et al.*, 1972). The most widely accepted classification in muscle biology is based on differences in the acid and alkaline stability of the myofibrillar ATPase reaction and distinguishes types I, IIA, IIB and IIC fibres (Brooke & Kaiser, 1970). This classification is performed from the visual comparison of three serial transverse muscle sections exposed to three different preincubation pH values (4.10, 4.35 and 10.4). Such a manual classification is extremely tedious and time consuming. To overcome this problem, Henckel (1989) proposed an image analysis system to type fibres as I, IIA and IIB from only one ATPase stain (pH 4.35), while type IIC was not considered. However, the latter fibres are important in some red mature muscles and during development (Suzuki & Cassens, 1980).

The depletion pattern of muscle glycogen strongly influences some aspects of meat quality (Monin, 1983, 1988). Muscular glycogen is heterogeneously distributed between myofibres and little is known about the post-mortem depletion of glycogen at the cellular level according to fibre types.

The present paper describes a computerized image analysis system which classifies myofibres from three ATPase stains as types I, IIA, IIB and IIC, exactly as described by Brooke & Kaiser (1970). The objective was to obtain percentage, mean area and relative area of each fibre type in a sample of muscle. In a second study, post-mortem glycogen depletion according to fibre types was investigated, using the same image analysis system.

## MATERIALS AND METHODS

### Histological methods

The samples used to develop the image analysis system were taken, within 45 min of slaughter, from the medial part of *semispinalis* muscle of five 100 kg BW Large White pigs. Samples were restrained on flat sticks with pins, promptly frozen in isopentane cooled by liquid nitrogen ( $-160^{\circ}\text{C}$ ) and stored at  $-80^{\circ}\text{C}$  until histological examination. Five serial  $10\ \mu\text{m}$  thick transverse muscle sections were obtained from each sample with a cryostat at  $-20^{\circ}\text{C}$ . One was stained in red with azorubine (reference stain), three were processed according to the myosin ATPase technique following preincubation at pH 4.10, 4.35 or 10.4 (Guth & Samaha, 1969; Brooke & Kaiser, 1970) and the last one was processed according to Pearse (1968) to reveal glycogen. Photographs of a representative serial cutting set are presented in Fig. 1.

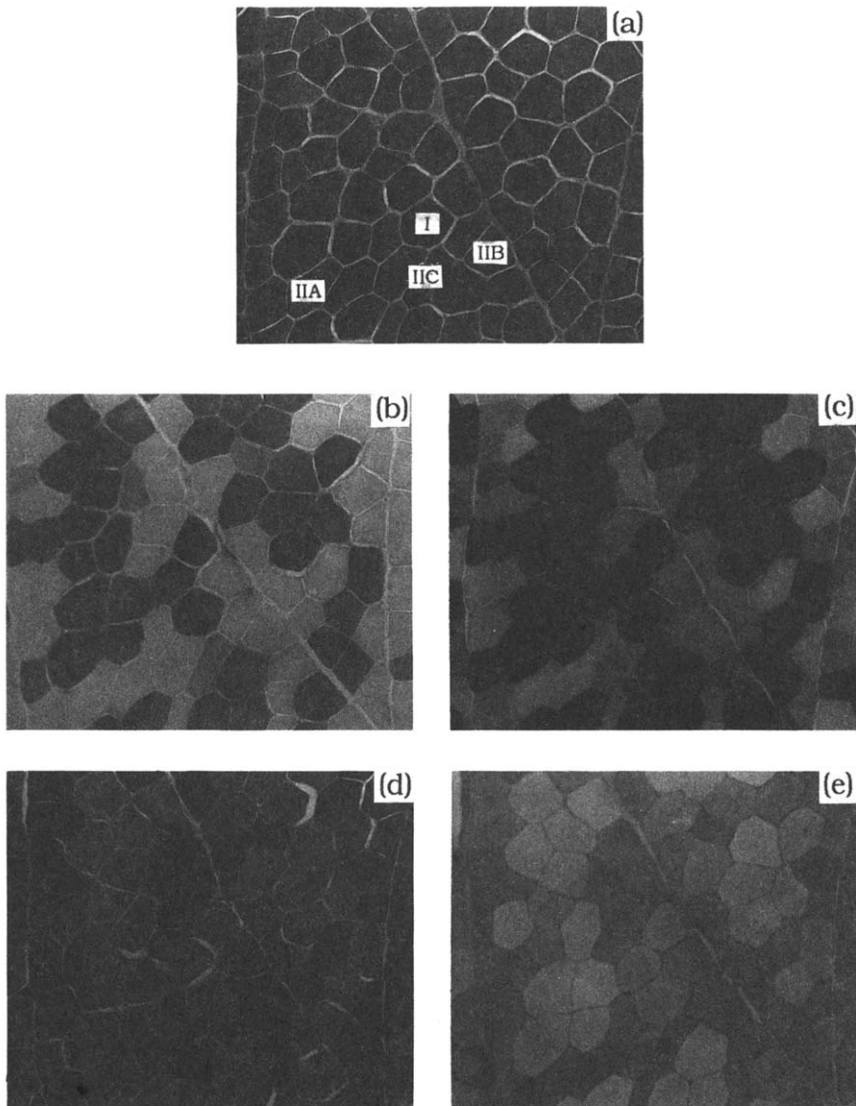


**Fig. 1.** Transverse serial frozen sections of *semispinalis* muscle from a 100 kg Large White pig. (a) Reference stain, (b, c, d) myosin ATPase stain after a preincubation at pH 4.10 (b), 4.35 (c), 10.4 (d) and (e) glycogen stain.

### System configuration

The operational system consisted of an optical microscope equipped with a CCD black and white camera (Sony AVC-D5CE), an image analysis board (Matrox MVP/VME) and a standard workstation computer (Sun 4/370, 32 Mb (Megabyte) central memory, 22 mips (machine instructions per second)) running under the UNIX system which controls all the image

analysis system. The image analysis board was composed of a graphic memory (1 Mb video RAM), an analogic–digital converter linked to the camera and a digital–analogic converter linked to a display output (monitor) to visualize the images. This system was plugged into the VME bus, an industrial standard allowing the connection between peripherals of the workstation, and was driven by the computer.

### **Image acquisition**

The five serial sections of a given set were digitized sequentially. Each field was represented by a  $512 \times 512$  pixel image (a 2D matrix). Each pixel ranged from 0 to 255, according to the luminance measured by the camera. The reference stain was first digitized using a green filter to enhance contrast between the fibre, stained in red, and the unstained interfibre material. Large structures belonging to the interfibre connective tissue network of the reference stain were interactively stored into a graphic memory to match the other stained sections coarsely. The operator then tried to match, as far as possible, these large structures with those present in the other stained sections of the set.

### **Individualization and classification of myofibres**

The full procedure has been described in detail by Buche (1990) and Buche & Camillerapp (1991). Four serial sections were used for each muscle sample. The first one (reference stain) was used to obtain a computerized image of the connective tissue network (delineation of cell limits). Computerized images of the connective tissue network of the other three sections were then partly extracted and automatically matched to the reference. Myofibrillar ATPase stain intensities were then estimated for each individual fibre, and used for fibre classification.

#### *Network extraction on the reference stain*

Computerized image extraction of the interfibre connective tissue network was performed to individualize each fibre. This network, on a monochromatic numerical image, was made up of thin interconnected branches. The automatic process included a global optimal thresholding step followed by a branch closing step (Buche *et al.*, 1989). The global thresholding was carried out by choosing the grey level which corresponded to the best luminosity gradient on an average on the entire image (Appendix 1). In the closing step, starting from the extremity of a branch, the algorithm determined the direction of the main inertial axis (Postaire, 1987) and searched for a pixel belonging to the network to close the branch between these two pixels (Denizon, 1986; Buche, 1990).

### Network matching

Matching of the reference network to the following stain networks was achieved using a polynomial transformation to take into account local distortions between the serial images (Mather, 1987; Buche, 1990; Buche & Camillerapp, 1991) (Appendix 2). Uniformly distributed landmark points were automatically generated from the ATPase stains and automatically paired to corresponding landmark points of the reference network to estimate the polynomial transformation (see Fig. 3).

### Measurements of fibre characteristics

After fibre individualization and matching, the system measured individual structural parameters (area, perimeter, shape =  $4 \text{ Pi area/perimeter}^2$ ) on the reference stain and luminances on the ATPase stains. Individual staining intensities were determined as the mean pixel luminance determined from  $n$  pixels around the central area of each fibre. For a given section, the factor  $n$  was chosen so that the measurement window was smaller than the smallest fibre. Two luminance threshold levels were determined interactively on each ATPase stain to define low, medium and high stain levels. The results were combined to generate types I, IIA, IIB and IIC fibres according to Fig. 2. Type I was defined as fibres exhibiting low stain after preincubation at pH 10.4. Fibres with low stain at pH 4.10 were classified as type IIA (low stain at pH 4.35) or IIB (medium stain at pH 4.35). All remaining fibres, with medium to high stain after all three preincubation pH treatments were defined as type IIC.

### Post-mortem glycogen depletion according to fibre types

Three samples of the *semispinalis* muscle from four Large White pigs of 100 kg liveweight were taken at 0, 1, 2, 4, 7 and 24 h *post mortem*. One sample

FIBRE TYPE \ pH	4.10	4.35	10.4
I	●	●	○
IIA	○	○	●
IIB	○	⊗	●
IIC	⊗ ●	⊗ ●	⊗ ●

Fig. 2. ATPase staining intensities of type I, IIA, IIB and IIC fibres according to preincubation pH. ● high; ⊗ medium; ○ low.

was immediately homogenized in 5 mM iodoacetate for measurement of pH. Another was frozen in liquid nitrogen and lyophilized to determine glycogen (Dalrymple & Hamm, 1973) and lactate (Bergmeyer, 1974) concentrations after homogenization in 0.5 M perchloric acid. The third sample was used to type myofibres as described above. As mentioned, glycogen stain intensity was determined on a serial transverse section in individual myofibres as the mean pixel luminance determined from  $n$  pixels around the central area of the fibre.

## RESULTS AND DISCUSSION

### Image acquisition

Before digitization, it was important to verify that the field to be studied was of good quality on the serial sections of a given set. The time needed to choose a field and digitize four stains (one reference and three ATPase stains) was 12 min.

### Network extraction

With the present system configuration, 3 min were needed for the automatic image extraction of the connective tissue network from the reference stain. A validation carried out on 13 reference stains showed that less than 2% of the septa were erroneous before interactive correction of residual errors (5–10 min). The optimal number of fibres per digitized field was between 200 and 300. Analysing more than 300 fibres would take too much time for interactive correction of the network.

### Network matching

Preliminary observations demonstrated that a rough matching, combining a movement of rotation and translation, as proposed by Henckel (1989), was insufficient. Indeed, 2–15% of fibres may be wrongly matched per stain, depending on the distortion between serial cuttings (Table 1). Distortion between two stains is actually the combination of translation plus rotation plus local distortions. Local distortions may be due to staining or cutting effects and to the random presence of adipocytes. A polynomial transformation of degree three was found to be sufficient to take into account local distortions (Fig. 3). At least 20 pairs of landmark points were needed on each stain for an accurate estimation of the coefficients of this polynomial transformation. An automatic matching process was used

**TABLE 1**

Percentage of Fibres (Means  $\pm$  SD) Wrongly Matched to the Reference Stain Before and After Polynomial Transformation

<i>Stains</i>	<i>Number of stains</i>	<i>Before polynomial transformation</i>	<i>After polynomial transformation</i>
ATPase 4·10	15	6·0 $\pm$ 4·3	1·2 $\pm$ 0·9
ATPase 4·35	15	3·8 $\pm$ 4·7	2·5 $\pm$ 2·4
ATPase 10·4	15	2·3 $\pm$ 3·0	1·7 $\pm$ 1·9

(Buche, 1990), which generates 200–300 landmark points per stain to estimate the coefficients of the polynomial transformation (Appendix 2). This procedure reduced the error to about 2% with a large reduction in variability (Table 1). An interactive procedure is available for correction of residual errors by moving, with a cursor, the badly matched centres of gravity. Automatic matching of the three ATPase stains to the reference and interactive correction took 7 and 12 min, respectively.

### Measurement of staining intensities and classification of myofibres

The uniformly distributed final reaction product of ATPase stains within a fibre (Fig. 1) allowed the measurement of the mean luminance around the central area of each fibre. The staining intensity of each fibre was automatically registered and stored in a file suitable for statistical analysis such as fitting frequency distributions or multivariate analysis. For each ATPase stain, luminance threshold levels could also be set interactively to type fibres according to Brooke & Kaiser (1970) (Fig. 2). This operation took 7 min per serial cutting set. After this step, an optional interactive procedure is available to change, with a cursor, the type of a given fibre wrongly

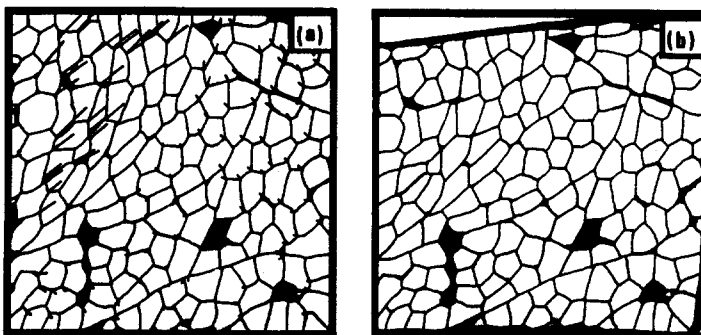


**Fig. 3.** Network polynomial transformation. (a) Before transformation, segments denote local distortions. (b) After transformation.



classified because of the presence of artefacts in the stain (e.g. specks of dye, small holes due to the formation of microscopic ice crystals while freezing the muscle sample).

### Use of the image analysis system for the study of post-mortem muscle glycogen depletion

Photometric determination of PAS (Periodic Acid Schiff) stain intensity in histochemical sections is an accurate method for the determination of glycogen content in individual muscle fibres (Halkjaer-Kristensen & Ingemann-Hansen, 1979; Vollestad *et al.*, 1984). As shown in Fig. 4, a significantly higher luminance, indicative of a lower glycogen concentration ( $P < 0.001$ ), was found in type I than in type II fibres immediately after slaughter. No difference between IIA and IIB fibres was observed. Luminance increased from slaughter in the type I fibres while it only increased from around 2 h in the type II fibres. Thereafter, a progressive increase took place in all fibre types up to around 7 h. Type I fibres, poorer in glycogen immediately after slaughter were completely depleted at 7 h *post*

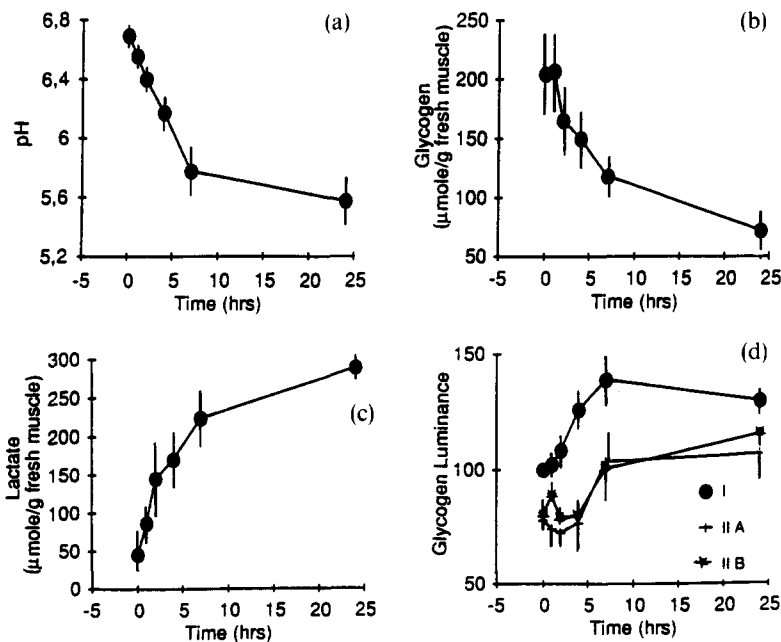


**Fig. 4.** Post-mortem changes in pH (a), glycogen (b) and lactate (c) concentrations and luminance of glycogen staining according to fibre types (d) in *semispinalis* muscle of 100 kg Large White pigs. Each point represents the mean of four animals and vertical bars indicate standard deviation.

*mortem*, whereas residual glycogen still remained in some type II fibres at 24 h *post mortem*. These results are in good agreement with those obtained with biochemical techniques on the same samples, i.e. decrease in pH and glycogen concentration and increase in lactate concentration with time (Fig. 4). With both histochemical and biochemical methods, post-mortem changes mainly occurred during the first 7 h *post mortem*.

To the authors knowledge, the present computerized image analysis system is the first one to take into account local distortions between serial sections and it can classify myofibres exactly as described by Brooke & Kaiser (1970) into types I, IIA, IIB and IIC. Overall, the complete analysis of four stains for the classification of 200–300 fibres required 10 min of batch processing and 36–41 min of interactive work (Table 2). The additional time

**TABLE 2**  
Time Required to Analyse a Cutting Set (Four Stains) for Classification of 200–300 Fibres with the Image Analysis System (Time Expressed in Minutes)

<i>Steps</i>	<i>Interactive work</i>	<i>Automatic calculation</i>
Digitization	12	
Network extraction		3
Network correction	5–10	
Network matchings	12	7
Fibre typing	7	
Total	36–41	10

needed for processing a fifth glycogen stain was 7 min of interactive work. The storage memory needed to analyse one serial cutting set (reference, three ATPase stains, one glycogen stain) was 2 Mb:  $5 \times 0.25 = 1.25$  Mb for digitized images and  $3 \times 0.25 = 0.75$  Mb for calculated images. The present system is an effective tool to type myofibres objectively according to Brooke & Kaiser's classification, describe post-natal muscle fibre development, qualitatively estimate glycogen at a cellular level according to fibre types and study the significance of morphological and physiological parameters of live pig muscles for meat quality. The use of the system for analysis of post-mortem glycogen depletion according to fibre type is very promising and deserves further investigation.

For more details, Buche's thesis and a full description of the algorithm are available by writing to P. Buche, INRA, Département d'Informatique, 11 rue Jean Nicot, 75007 Paris, France.

## ACKNOWLEDGEMENTS

The authors wish to thank Dr M. Bonneau for critical evaluation of the manuscript and Dr G. Monin for glycogen and lactate determinations. They would also like to acknowledge P. Mauclair, P. Loret, E. Ricros and A. Blandin for their helpful contribution to the development and validation of the program.

## REFERENCES

- Ashmore, C. R. & Doerr, L. (1971). *Exp. Neurol.*, **30**, 431.
- Bergmeyer, H. V. (1974). *Methods of Enzymatic Analysis*. Academic Press, New York.
- Brooke, M. H. & Kaiser, K. K. (1970). *Arch. Neurol.*, **23**, 369.
- Buche, P. (1990). *RACINE: Un système d'analyse multi-images de coupes sériées. Application à la caractérisation de fibres musculaires*. Thesis, Rennes I University, France.
- Buche, P. & Camillerapp, J. (1991). *Ann. Conf. Eur. Assoc. Computer Graphics*. Vienna.
- Buche, P., Lefaucheur, L. & Mauclair, P. (1989). In *XXI Journées de Statistiques*. Rennes, France.
- Dalrymple, R. M. & Hamm, R. (1973). *J. Food Technol.*, **8**, 439.
- Denizon, A. (1986). *Etude de la texture musculaire par traitement numérique d'images*. Thesis, Clermont-Ferrand II University, France.
- Guth, L. & Samaha, F. J. (1969). *Exp. Neurol.*, **28**, 365.
- Halkjaer-Kristensen, J. & Ingemann-Hansen, T. (1979). *Histochem. J.*, **11**, 629.
- Henckel, P. (1989). In *Proc. 40th Annual Meeting EAAP*. Dublin, Eire.
- Lefaucheur, L. (1990). *INRA Prod. Anim.*, **2**, 205.
- Mather, P. M. (1987). *Computer Processing of Remotely-sensed Images; an Introduction*. Wiley, Chichester.
- Monin, G. (1983). *J. Rech. Porcines France*, **15**, 151.
- Monin, G. (1988). *J. Rech. Porcines France*, **20**, 201.
- Pearse, A. G. E. (1968). *Histochemistry: Theoretical and Applied*. Little, Brown & Co., Boston.
- Peter, J. B., Barnard, R. J., Edgerton, V. R., Gillespie, C. A. & Stempei, K. E. (1972). *Biochemistry*, **11**, 2627.
- Postaire, J. G. (1987). In: *De l'image à la décision*. Dunod Informatique, Paris.
- Suzuki, A. & Cassens, R. G. (1980). *J. Anim. Sci.*, **51**, 1449.
- Vollestad, N. K., Vaage, O. & Hermansen, L. (1984). *Acta Physiol. Scand.*, **122**, 433.

## APPENDIX 1: THE AUTOMATIC GLOBAL THRESHOLDING FOR CONNECTIVE TISSUE NETWORK EXTRACTION ON THE REFERENCE STAIN

The Sobel filter was used to obtain the gradient image as follows:

For a given pixel called \*:

$$\begin{array}{ccc} A3 & A2 & A1 \\ A4 & * & A0 \\ A5 & A6 & A7 \end{array}$$

with  $A_0, \dots, A_7$  corresponding to the grey level (0–255) of each neighbouring pixel, the gradients in the X and Y directions were first calculated.

$$\text{grad X} = (A_1 + 2A_0 + A_7) - (A_3 + 2A_4 + A_5)$$

$$\text{grad Y} = (A_3 + 2A_2 + A_1) - (A_5 + 2A_6 + A_7)$$

Then, the gradient value was determined:

$$\text{grad} = ((\text{grad X}^2 + \text{grad Y}^2)/32)^{1/2}$$

The global thresholding algorithm included the following four steps.

- (1) Determination of the gradient value (grad) for each pixel on the reference stain.
- (2) Calculation of the main gradient for each grey level.
- (3) The global threshold was defined as the grey level associated with the higher mean gradient.
- (4) All the pixels of the image whose grey level were lower than the threshold value were considered as background and the other ones as pixels belonging to the connective tissue network.

## APPENDIX 2: THE MODEL FOR THE POLYNOMIAL TRANSFORMATION

$S_1$  and  $S_2$  are the coordinates of a set of  $n$  points on the two images to be matched:

$$S_1 = (X_{1i}, Y_{1i}), \quad i \in (1, \dots, n) \text{ in image 1}$$

$$S_2 = (X_{2i}, Y_{2i}), \quad i \in (1, \dots, n) \text{ in image 2}$$

where  $(X_{1i}, Y_{1i})$  is the point in image 1 which corresponds to  $(X_{2i}, Y_{2i})$  in image 2. Finding the geometrical transformation consists of estimating the polynomial transformation which gives a set of points from the other one. If we call:

$$S'_2 = (X'_{2i}, Y'_{2i}), \quad i \in (1, \dots, n)$$

the set of points resulting from the application of the transformation to the set of points  $S_1$ , the following correspondence is obtained:

$$\begin{aligned} X'_{2i} &= f(X_{1i}, Y_{1i}) \\ Y'_{2i} &= g(X_{1i}, Y_{1i}) \end{aligned}$$

with  $f$  and  $g$  two polynomial functions of degree  $m$ ,  $m > 1$ . Two independent polynomial transformations in the  $x$  and  $y$  directions were applied to provide a more flexible model. For example, for  $m = 2$ , we have:

$$X'_{2i} = a_1 + a_2 X_{1i} + a_3 Y_{1i} + a_4 X_{1i} Y_{1i} + a_5 X_{1i}^2 + a_6 Y_{1i}^2$$

The components of the squared Euclidean distance between the observed points  $(X_{2i}, Y_{2i})$  and the estimated ones  $(X'_{2i}, Y'_{2i})$  are given by:

$$d_{X_i} = (X_{2i} - f(X_{1i}, Y_{1i}))^2 \quad \text{and} \quad d_{Y_i} = (Y_{2i} - g(X_{1i}, Y_{1i}))^2$$

Summing up over  $n$  points gives the following expressions which are then minimized independently:

$$D_X = \sum_{i=1}^n d_{X_i} \quad \text{and} \quad D_Y = \sum_{i=1}^n d_{Y_i}$$

using the least squares method. For more details, see Buche (1990) and Buche & Camillerapp (1991).